

# Tissue Factor–Activated Coagulation Cascade in the Tumor Microenvironment Is Critical for Tumor Progression and an Effective Target for Therapy

Yuan Liu<sup>1</sup>, Pengfei Jiang<sup>1</sup>, Katerina Capkova<sup>2</sup>, Dong Xue<sup>1</sup>, Longwu Ye<sup>1</sup>, Subhash C. Sinha<sup>3</sup>, Nigel Mackman<sup>4</sup>, Kim D. Janda<sup>2</sup>, and Cheng Liu<sup>1</sup>

## Abstract

Tissue factor (TF), a rate-limiting enzyme cofactor in activating coagulation, is highly expressed in a wide spectrum of human tumor and tumor stromal cells. Using TF-deficient cancer cells and a conditional TF-knockout mouse model, we show that TF expressed by cancer cells, but not by the host stromal cells, plays a critical role in tumor growth. In the tumor microenvironment, serum coagulation factors are readily extravasated and therefore lead to continuous TF-mediated activation of coagulation proteases. To target this highly specific cascade of serine proteases, we used both a TF:FVIIa inhibitor and doxorubicin-based prodrugs that are selectively activated by TF:FVIIa, FXa, and thrombin. Treatment with the TF:FVIIa inhibitor led to growth retardation in breast tumor models. In contrast, treatment with the prodrug eliminated primary tumor cells and lung metastases without apparent toxicity. Our findings offer preclinical proof of principle that targeting the coagulation cascade that is activated in the tumor microenvironment can be a highly effective approach for cancer therapy. *Cancer Res*; 71(20); 6492–502. ©2011 AACR.

## Introduction

Tissue factor (TF) is the plasmalemma receptor and obligatory cofactor for cell surface assembly and initiation of the coagulation protease cascade (1). It is widely expressed and a key determinant of tumor progression (2–6). In addition to its function as an initiator of hemostasis, TF can signal through TF:FVIIa, FXa, and thrombin-mediated activation of protease-activated receptors. Human TF is a glycoprotein of 263 residues, which shares structural homology with the cytokine receptor families (7–9). To initiate the coagulation protease cascade, TF binds and facilitates activation of factor VII(FVII) to the serine protease factor VIIa(FVIIa) and allosterically conforms the catalytic site of the bound FVIIa and associates with the physiologic substrate zymogens factor X(FX) and factor IX (10, 11), leading to thrombin generation, fibrin deposition, and platelet activation. TF presence is prominent in the perivascular cells that form a hemostatic barrier and serve to limit hemorrhage after vessel injury. Therefore,

TF-mediated coagulation is otherwise inactive elsewhere in the body, unless there is an injury to the vasculature.

To assess the role of TF in tumor progression, we generated TF knockout cancer cells by crossing a PyVmT mouse with TF flox/flox mice. Multiple cancer lines were established from the tumors developed in TF<sup>flox/flox</sup>-PyVmT(+) mice. In addition, TF knockout was achieved by infecting the established TF<sup>flox/flox</sup>-PyVmT(+) tumor cell line with adenovirus vector express Cre recombinase. The contribution of the host TF was evaluated in TF<sup>flox/flox</sup> LysM Cre(+) mice with the deleted TF gene in mature macrophages and granulocytes, and the TF<sup>flox/flox</sup> Tie2 Cre(+) mice specifically deleted TF gene in endothelial cells and hematopoietic cells. Through these genetic models, we show that TF expressed by cancer cells is the key contributor to tumor growth, but not the host TF expressed by myeloid cells and endothelial cells.

Because of enhanced tumor vasculature permeability, the coagulation factors and albumin are extravasated and present in the tumor microenvironment where the coagulation cascade is constantly activated by the high level of the tissue factor on the tumor and stromal cell surface. Fibrin deposit in tumor stroma is commonly observed. Therefore, the coagulation cascade is an attractive target for prodrug therapy. Peptide conjugates of doxorubicin designed for activation by plasmin (12, 13) and cathepsins (14, 15) have been described. Indeed, the TF:FVIIa and proteases in the coagulation cascade have the highest substrate specificity among serine proteases and are very well characterized (16, 17). We synthesized 2 types of doxorubicin prodrugs targeting coagulation proteases. The first type of prodrug contained a short polyethylene glycol or a succinyl substituent to enhance the prodrug

**Authors' Affiliations:** Departments of <sup>1</sup>Immunology and Microbial Science, <sup>2</sup>Chemistry, <sup>3</sup>Molecular Biology, The Scripps Research Institute, La Jolla, California; <sup>4</sup>Division of Hematology/Oncology, University of North Carolina at Chapel Hill, Chapel Hill, North Carolina

**Note:** Supplementary data for this article are available at Cancer Research Online (<http://cancerres.aacrjournals.org/>).

**Corresponding Author:** Cheng Liu, The Scripps Research Institute, 10550 North Torrey Pines Road, La Jolla, CA 92037. Phone: 858-785-7734; Fax: 858-785-7756; E-mail: [chengliu@scripps.edu](mailto:chengliu@scripps.edu)

**doi:** 10.1158/0008-5472.CAN-11-1145

©2011 American Association for Cancer Research.

solubility, while the second prodrug includes an albumin binding  $\epsilon$ -maleimidocaproic acid (EMC) moiety to prolong half-life. The prodrugs were prepared by incorporating a small peptide appended to the amino functionality of doxorubicin resulting in an inactive compound, unless hydrolyzed to leucine-doxorubicin by TF:FVIIa and proteases within the coagulation cascade. Both types of prodrugs were found to be effective against primary tumors. However, the EMC containing prodrug showed superior efficacy as a single agent. *In vivo* administration of the EMC prodrug achieves complete tumor growth arrest and size reduction in the aggressive 4T1 murine mammary carcinoma. This strategy is similar to the cell-impermeable prodrug activation by cell surface-associated legumain in tumors (18, 19). The prodrugs significantly reduced the number of established lung metastasis and resulted in tumor eradication in human breast cancer xenograft. The coagulation protease activated prodrugs were stable in plasma indicating that the activation of coagulation is discreet and only occurs in the tumor microenvironment and during injury. Taken together, these data support that coagulation cascade is activated in the tumor microenvironment and may serve as an enzymatic target to achieve chemotherapeutic eradication of cancer and metastasis.

## Materials and Methods

### Reagents and cell lines

Biotinylated mouse TF antibody was purchased from American Diagnostica. Rabbit FVII antibody and human albumin were from Abcam. FVIIa and FXa were from HTI. Thrombin was from R&D systems. Doxorubicin and biotinylated albumin were from Sigma. Tissue factor was kindly provided by Wolfram Ruf. The 4T1 and MDA-MB231 cell lines were purchased from American Type Culture Collection (ATCC) and were characterized according to ATCC instructions. The cells were maintained in RPMI-1640 or Dulbecco's modified Eagle's medium supplemented with 10% FBS in a humidified incubator containing 5% CO<sub>2</sub> at 37°C. All the cell lines were used within 20 passages.

### Immunochemical analysis

4T1 and PyVmT tumor sections were stained by using biotinylated anti-TF and Goat anti-FVII antibody. Fluorescein streptavidin and Texas red were used as the secondary reporting reagent. FVII was i.v. injected into mice to increase FVII extravasation. Bio-Rad Radiance 2100 laser scanning confocal microscope was used for analysis.

### Albumin extravasation assay

Albumin or biotinylated albumin (30  $\mu$ mol/kg) was i.v. injected into the tail vein for observation. Fluorescein avidin was used for biotinylated albumin staining. Nuclei were stained with 4',6-diamidino-2-phenylindole (DAPI).

### Tissue distribution

Drug auto fluorescence was observed 12 hours after 10  $\mu$ mol/kg i.v. injection. Nuclei were stained with DAPI. Tissues was homogenized and diluted with 50% ethanol

containing 0.6 mol/L HCL. After normalization of protein concentration, the relative fluorescent intensity was measured by using of a Perkin-Elmer LS-50-B spectrofluorometer (excitation: 470 nm; emission: 590 nm).

### Colony-forming cell assays

Bone marrow single cell suspension was ( $1 \times 10^6$  per mL) cultured in MethoCult medium containing SCF, IL-3, and IL-6 (Stemcell Technologies) for 10 days at 37°C and 5% CO<sub>2</sub> and the number of colony are counted.

### Plasma pharmacokinetics

Blood from mice injected with 15  $\mu$ mol/kg prodrugs i.v. were collected at 10 minutes, 6-, 12-, and 24-hour postinjection and 1:10 diluted. Samples were measured by spectrofluorometer (excitation: 470 nm; emission: 590 nm).

### Mouse tumor models

PyVmT murine breast carcinoma was produced by injection of  $5 \times 10^5$  TF normal and deficient PyVmT tumor cells into the right flank of wild or conditional knockout C57BL/6J mice. 4T1 murine breast carcinoma model was produced by injection  $1 \times 10^6$  4T1 cells into the s.c. site on the back of BALB/c mice. MDA-MB231 human breast carcinoma model was generated by injection of  $1 \times 10^6$  MDA-MB231 cells into the s.c. site on the back Hsd:Athymic nude mice. Treatment was initiated when the tumors reached 4 mm in diameter through intraperitoneal (i.p.) injections of the indicated reagents. The lungs were removed on day 24 and fixed in the Bouin's solution to count spontaneous lung metastases. Number of lung metastases was counted under an anatomy microscope. Experimental lung metastases were induced by i. v. injection of  $2 \times 10^6$  4T1 in the tail vein of BALB/c mice. EMC-LTPRL-DOX treatment was started on day 16 with i.p. injection of 15  $\mu$ mol/kg daily. Experimental lung metastases were count on day 25. Tumor growth (volume = length  $\times$  width  $\times$  width/2) and signs of physical discomfort were monitored including for any gross evidence of tumor necrosis, local tumor ulceration, and evidence of toxicity including the mobility of animals, response to stimulus, piloerection, eating, and weight. These procedures have been reviewed and approved by the Institutional Animal Care and Use Committee at The Scripps Research Institute.

### Statistical analysis

Statistical significance of data was determined by the 2-tailed Student *t* test.

## Results

### TF activates coagulation within the tumor microenvironment

To determine cancer cell-surface expression of TF:FVIIa complex, we examined 4T1 murine syngeneic mammary carcinoma and polyoma virus middle T antigen (PyVmT) murine spontaneous mammary carcinoma by immunohistochemical analysis using the rabbit anti-mouse TF antibody. The staining shows that there is high-level expression of the

TF on 4T1 tumor cell surface (Fig. 1A). It also shows that FVII can be extravasated readily from the vessel into the tumor microenvironment of primary tumors and TF:FVIIa complex are detectable on the tumor cell surface (Fig. 1B and 1C). The TF expression was furthermore found on the cell face of tumor associated macrophage in PyVmT tumor (Fig. 1D). Expression of TF is also confirmed by Western blot analysis (Fig. 1E). A schematic presentation of TF:FVIIa complex formation in primary tumor microenvironment is proposed (Fig. 1F). On the basis of the size of the coagulation factors and the enhanced permeability of tumor vasculature (Supplementary Table S1), FVII and FX extravasate from leaky tumor vessels into the tumor microenvironment of primary tumors and bind to the cell surface TF to active coagulation cascade.

#### Albumin readily extravasates from the tumor vasculature into tumor microenvironment

To further evaluate the enhanced permeability of tumor vascular of serum proteins, we examined the extravasation of albumin by injecting biotinylated albumin into circulation of tumor-bearing mice. Albumin and biotinylated albumin (30  $\mu\text{mol/kg}$ ) were i.v. injected into the tail vein of tumor-bearing mice. Tumor and normal organ specimens were collected and frozen sections were probed with Fluorescein isothiocyanate-labeled streptavidin to visualize the biotinylated albumin. Albumin is readily extravasated in tumor, but not in normal organs such as liver (Fig. 1G). In tumor tissue, biotinylated albumin is accumulated in the tumor microenvironment

(Fig. 1G, tumor), but absent in normal liver (Fig. 1G, liver) and other organs (data not shown).

#### TF overexpression is a critical mediator of the tumor growth

A transgenic animal expressing the polyoma virus middle T antigen (PyVmT) is a robust breast cancer model developing multiple palpable mammary carcinomas spontaneously. To generate TF knockout cancer cells, we crossed TF<sup>+/+</sup>-PyVmT (+) mice with TF<sup>lox/lox</sup>-PyVmT(-) mice to acquire TF<sup>lox/lox</sup>-PyVmT(+) mice (Supplementary Fig. S1A). The mouse tail PCR genotyping were performed to confirm TF<sup>lox/lox</sup>-PyVmT(+) mice (Supplementary Fig. S1B). TF<sup>lox/lox</sup>-PyVmT(+) cancer cell lines were established from the spontaneous tumors developed in TF<sup>lox/lox</sup>-PyVmT(+) mice. The TF<sup>-/-</sup> PyVmT(+) cancer cell line was achieved by infecting the established TF<sup>lox/lox</sup>-PyVmT(+) tumor cell line with adenovirus vector expressing Cre recombinase and GFP+ marker (Supplementary Fig. S1C). The Cre recombinase eliminates a segment of TF gene from the genome and disrupts TF expression completely (Supplementary Fig. S1D).

To examine the role of TF expressed by cancer cell in tumor growth, TF normal (TF<sup>+/+</sup>-PyVmT+) and TF-deficient (TF<sup>-/-</sup>-PyVmT+) tumor cells were inoculated into C56BL/6 mice. The tumor induced by TF-deficient cells grow much slower than that induced by TF normal cells (Fig. 2A and B). TF-deficient cells only developed and grew small tumors in mice, indicating a critical role of TF in tumor progression.

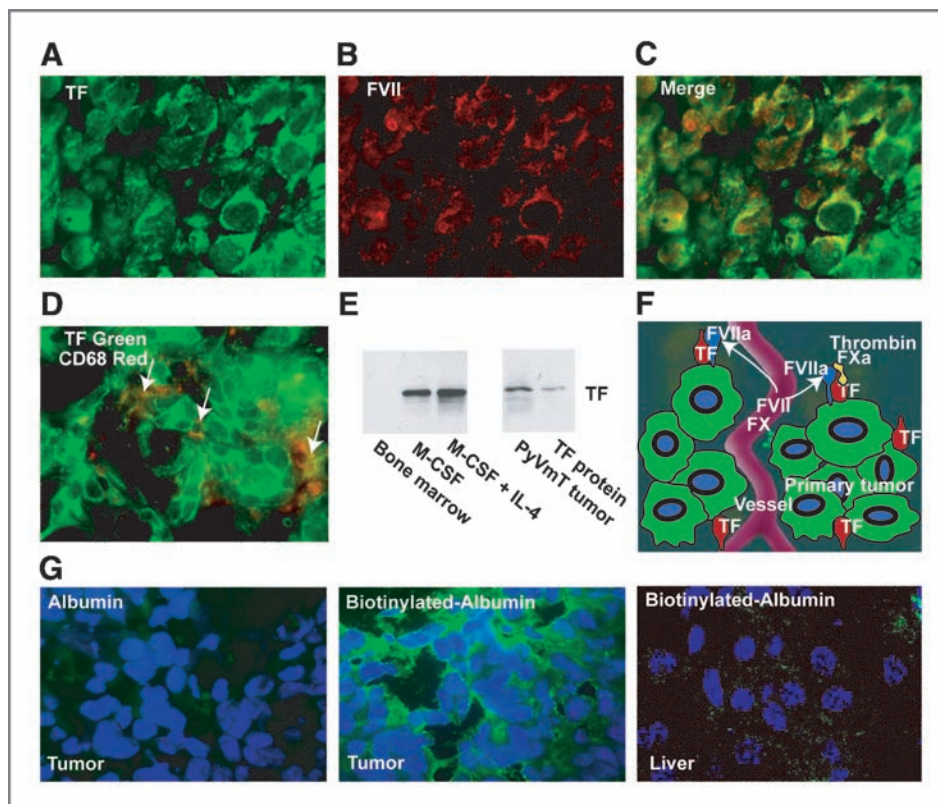


**Figure 1.** TF:FVIIa complex is formed on cell surface in the tumor microenvironment. TF (A, green) and FVII (B, red) is detected on 4T1 tumor cell surface. TF and FVIIa are colocalized (C, yellow). TF (D, green) is also observed on cellular surface of PyVmT tumor cells and tumor-associated macrophages (red, CD68). E, Western blotting of TF expression. F, schematic presentation of extravasation of coagulation factors. G, assessment of albumin extravasation with fluorescein-labeled streptavidin (green).

Hematoxylin and eosin (H&E) staining of tumor specimens indicated the TF-deficient tumors contain scarce and small lobular of tumor cells, but abundance of stromal component between tumor cells (Supplementary Fig. S1E).

The contribution of TF expressed by stromal cells was evaluated in mice with conditional TF gene knockout in different host cells. We have transplanted TF normal cancer cells into the  $TF^{lox/lox}$ .LysM Cre(+) mice in which TF gene is deleted in mature macrophage and granulocyte, and the  $TF^{lox/lox}$ .Tie2 Cre (+) mice in which TF gene deleted endothelial cells and hematopoietic cells. We found no difference in tumor growth patterns in these models, and all the tumor volume are larger than  $1,200 \text{ mm}^3$  (Fig. 2C and D). However, when we transplanted  $TF^{-/-}$  cancer cells into the  $TF^{lox/lox}$ .LysM Cre(+) and Tie2 Cre (+) mice, tumor growth is retarded and all the tumor volume is less than  $600 \text{ mm}^3$  (Fig. 2E and F). TF deletion in stromal cells does not seem to suppress tumor growth. Taken together these results indicate that TF expressed by cancer cells plays a significant role in tumor progression, in contrast to TF provided by stromal cells.

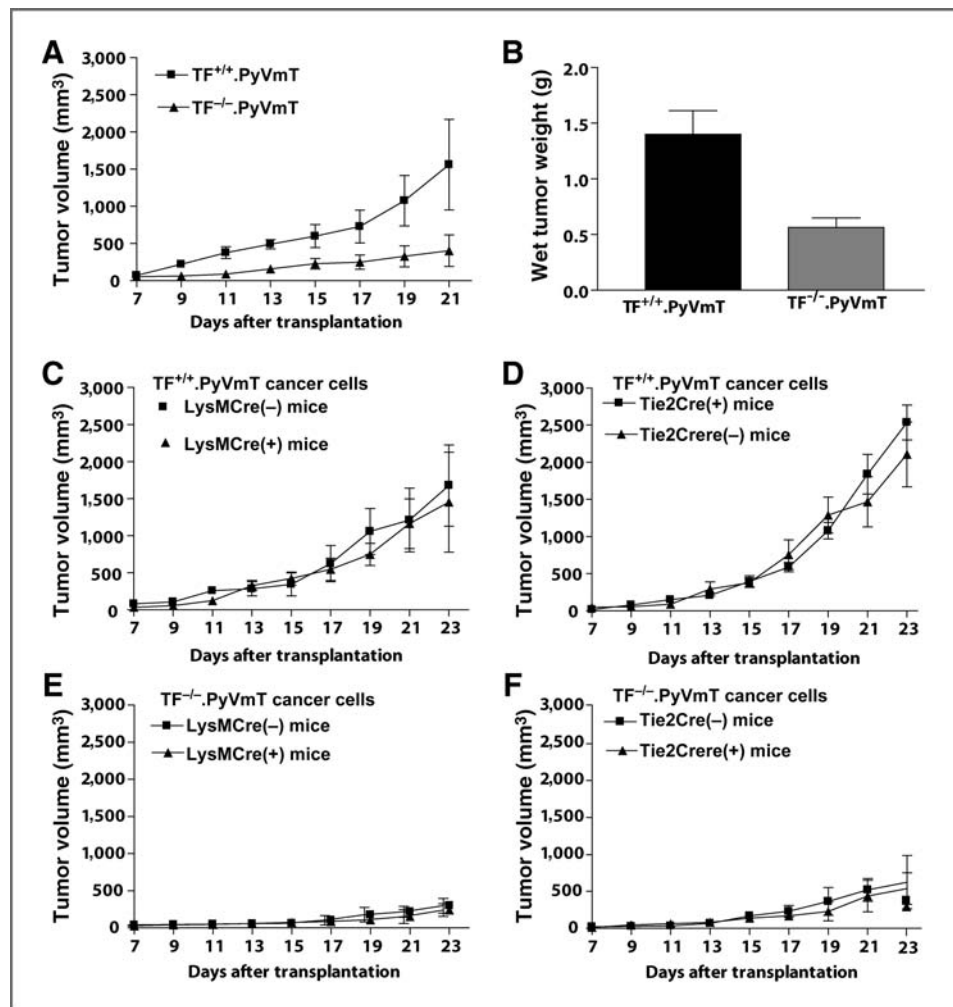
### FVIIa inhibitor suppresses tumor growth

To evaluate the role of TF:FVIIa on tumor growth, a reported high-affinity inhibitor of FVIIa (Supplementary Fig. S2A) was synthesized and applied in to 4T1 *in vivo* model with 0.2 mg/kg dosage daily. At this dose, bleeding time was prolonged 3-fold (Supplementary Fig. S2B) in mouse tail-bleeding experiment. The FVIIa inhibitor had an inhibitory effect on tumor growth (Supplementary Fig. 2C) that is consistent with the role of TF:FVIIa activity in tumor growth. However, the FVIIa inhibitor has a low solubility and short half-life in blood. The lack of more pronounced effects is due to the poor pharmacokinetic properties of this compound. These experiments underscore the difficulty in the development of successful inhibitors for this class of serine proteases in cancer therapy, especially due to the risk of bleeding.

### Synthesis of doxorubicin-based prodrugs

To validate the strategy of tumor microenvironment activated prodrugs and to take advantage of an enhanced vascular permeability of the blood vessels found in malignant tissue for circulating macromolecules, we synthesized 2 doxorubicin

**Figure 2.** TF deletion in cancer cell suppresses tumor growth. A, tumor growth and tumor weight (B) of mice planted with TF deficient and TF  $+/+$  PyVmT cells. Tumor growth in wild and TF conditional knockout mice that were planted with TF  $+/+$  (C, D) and TF  $-/-$  (E, F) PyVmT cancer cells.



prodrugs targeting coagulation proteases containing: (a) a short polyethylene glycol substituent to enhance the prodrug solubility, (b) an albumin binding  $\epsilon$ -maleimidocaproic acid moiety introduced to react with cysteine-34 of the albumin circulating in the bloodstream, increasing the prodrug half-life, and significantly reducing drug toxicity. The plasma protein albumin preferentially accumulates in solid tumors (20, 21), and can be used as an endogenous drug carrier to enhance the pharmacologic properties of these drugs. The synthesis of both prodrugs commenced with the preparation of peptides 2a–b using standard Fmoc solid phase synthesis,

where 2-(2-methoxyethoxyacetic acid) or  $\epsilon$ -maleimidocaproic acid was incorporated as the last amino acid residue in the growing sequence. After cleavage from the resin, these peptides were purified by RP HPLC. Subsequent coupling with doxorubicin in the presence of PyBOP and diisopropylethylamine afforded the target prodrugs a and b, which were purified by RP HPLC and characterized by HR MS (Fig. 3A).

The activation of Peg-LTPRL-DOX by FVIIa and TF:FVIIa was carried out *in vitro* and analyzed by LC-MS (Fig. 3B and C). In the control sample, there was only 1 component, the Peg-LTPRL-DOX (WM 1240.5; ref. Fig. 3C, peak 2). Hence,

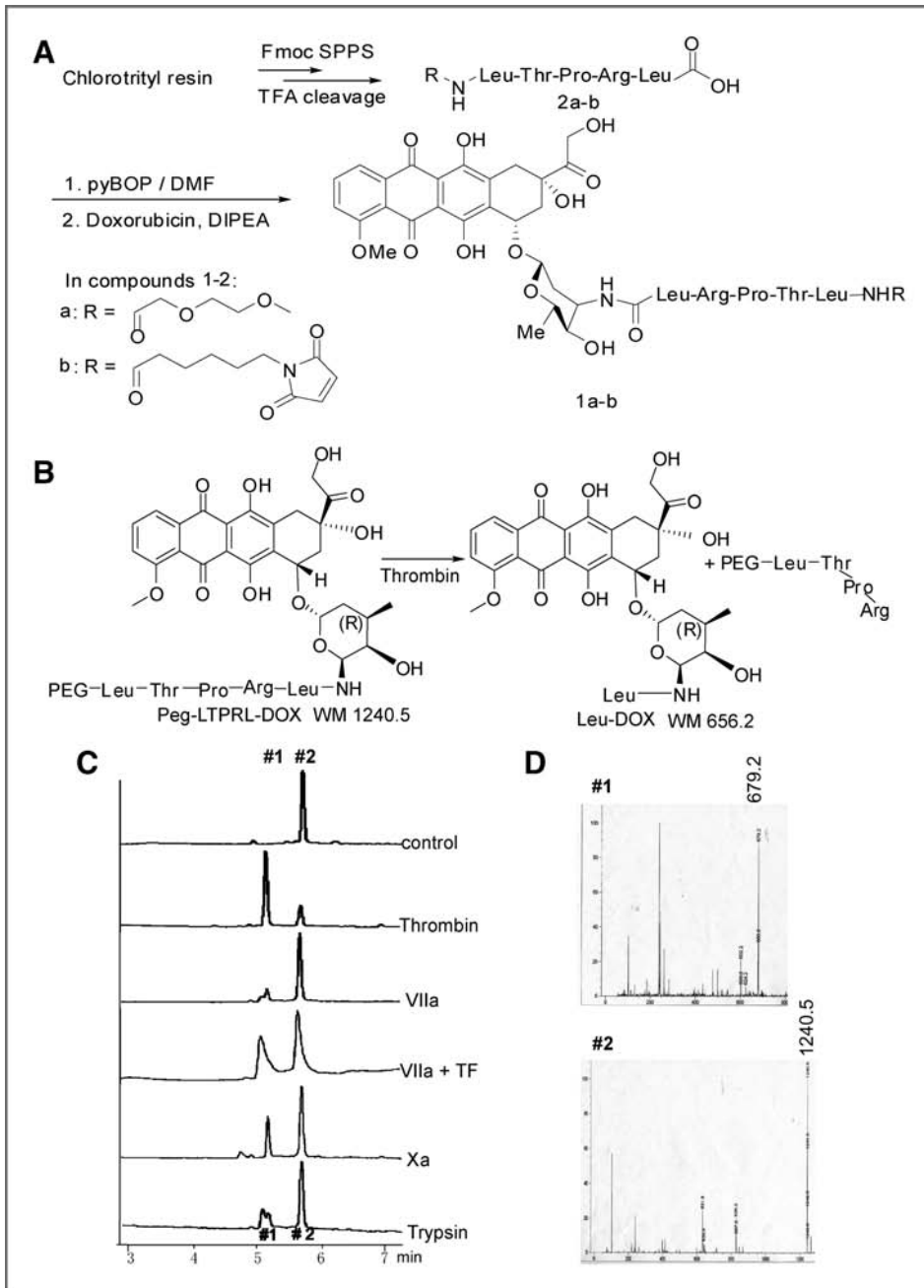


**Figure 3.** Prodrug synthesis and activation. **A**, synthesis scheme. **B**, scheme of prodrug activation. **C**, analysis of prodrug activation. **D**, peak 1 and peak 2 are prodrug and activated prodrug (+Na<sup>+</sup>), respectively.

**Table 1.** Steady-state kinetic constants for activation enzymes

Enzyme	$K_m$ (nmol/L)	$k_{cat}$ ( $\text{min}^{-1}$ )	$k_{cat}/K_m$ ( $\text{min nmol/L}^{-1}$ )
Thrombin	989	169.38	0.142
VIIa	1,887	8.94	0.004
VIIa+TF	1,423	16.08	0.011
Xa	1,558	4.32	0.003
Trypsin	2,106	3.42	0.001

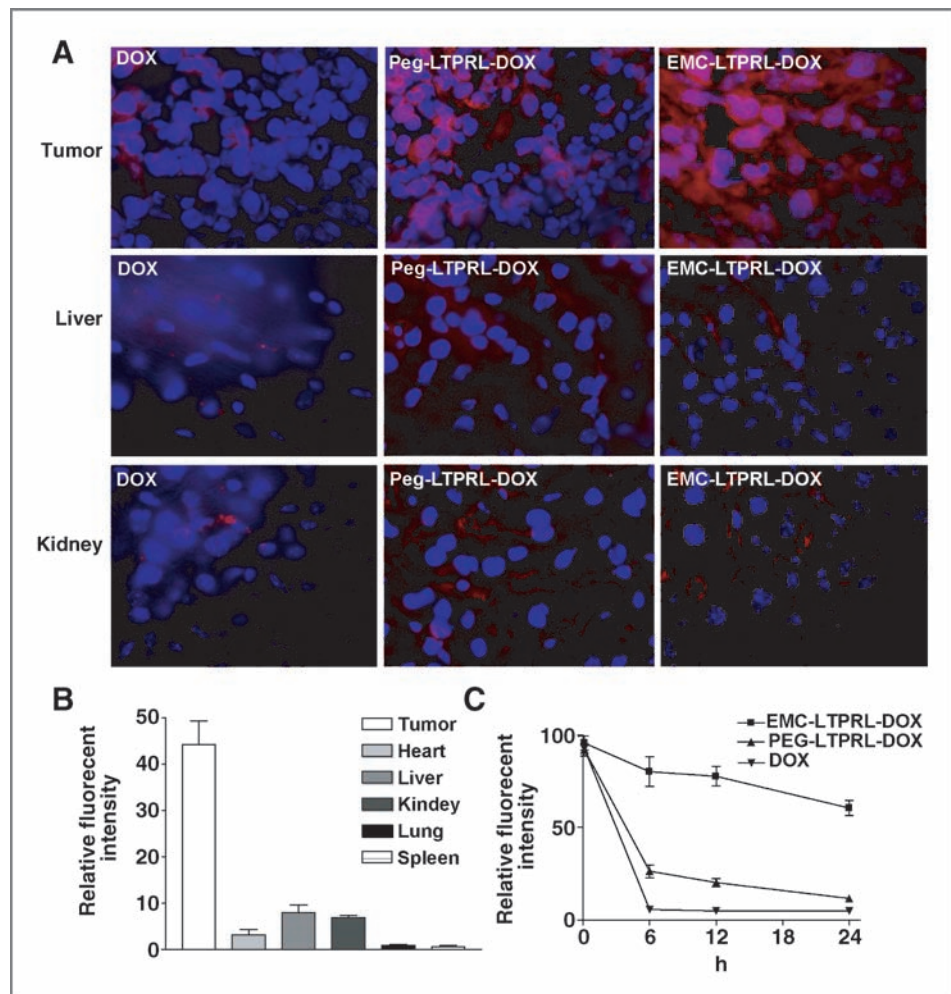
incubation of Peg-LTPRL-DOX with thrombin, FVIIa, and FXa induced activation of the prodrug producing Leu-DOX (WM 542.5; Fig. 3C, peak 1), which could be separated by liquid chromatography and detected by mass spectrometry (Fig. 3D). Inclusion of equal molar soluble TF extracellular domain with FVIIa significantly enhanced the activity of FVIIa as expected. However, this still underestimates the catalytic activity of TF: FVIIa complexes on the cell surface that are of native TF proteins and in an appropriate cell-surface lipid environment.

Indeed, nonspecific serine protease trypsin has a very low activity toward this prodrug. Although the catalytic efficiency of the serine proteases in the coagulation cascade and trypsin toward prodrug activation were determined (Table 1) and support the specificity of activation of the prodrug by serine proteases in the coagulation cascade.

### Prodrug activation and accumulation are enhanced in tumor

The profile of prodrug distribution and activation *in vivo* were determined by detecting prodrug and parent drug using a fluorescent microscope and a fluorometer. Prodrug and active prodrug accumulation were visualized in tumor sections after i.v. injection of 10  $\mu\text{mol/kg}$  DOX, Peg-LTPRL-DOX, and EMC-LTPRL-DOX, respectively (Fig. 4A, red color). The accumulation of the prodrug in tumors of Peg-LTPRL-DOX-treated mice and EMC-LTPRL-DOX-treated mice was greatly enhanced compared with that of doxorubicin-treated mice. Doxorubicin is cell permeable and has a high-clearance rate in tumor tissue, because doxorubicin is a small molecular compound. The EMC-LTPRL-DOX is cell impermeable until activated and is not taken up by normal tissue cells. The

**Figure 4.** *In vivo* distribution of prodrugs. A, autofluorescence of prodrugs (red) in samples. EMC-LTPRL-DOX showed nuclear positivity in tumor tissue. B, biodistribution of EMC-LTPRL-DOX. C, plasma pharmacokinetics of prodrugs.



fluorescence signal in the liver and kidneys of mice treated with EMC-LTPRL-DOX were primarily extracellular, suggesting that EMC-LTPRL-DOX is not activated in the normal tissues (Fig. 4A, liver and kidney). Nuclear positivity of active EMC-LTPRL-DOX is detected in tumor indicating that the prodrugs are only activated in the tumor microenvironment (Fig. 4A, tumor). Tumor accumulation and activation of the EMC-LTPRL-DOX are supported by quantitative assay in tumor-bearing mice (Fig. 4B). Binding to albumin (half-life 9–12 days) with EMC group, EMC-LTPRL-DOX shows a longer half-life in mouse circulating blood than that of doxorubicin, which almost disappeared after 6 hours from injection (Fig. 4C).

### Coagulation cascade serine protease-activated prodrug has low toxicity and is stable in serum

First, we assessed the stability of the prodrug compounds by mixing the Peg-LTPRL-DOX with mouse serum and incubated at 37°C for 24 hours. The compounds were subjected to HPLC analysis at the end of incubation (Fig. 5A) and the prodrugs appeared very stable in serum and only minor degradation products were observed that was distinct from activated drug. With 3 mg/kg injection every 2 days, doxorubicin caused significant toxicity as shown by weight loss (Fig. 5B) whereas both Peg-LTPRL-DOX and EMC-LTPRL-DOX lacked apparent toxicity and weight loss. We further evaluated the effect on white blood cells by EMC-LTPRL-DOX prodrug and compared this with doxorubicin (Supplementary Table S2). Single injection of doxorubicin at MTD caused significant WBC reduction,

whereas EMC-LTPRL-DOX given at a "save-dosage" had no effect on the WBC count. Next, we examined the effect of EMC-LTPRL-DOX on hematopoietic stem cells using a colony forming assay. Doxorubicin showed significant suppression on the formation of CFU-GM. In contrast, EMC-LTPRL-DOX at the same concentration had no effect on colony formation (Fig. 5C) indicating the coagulation cascade is not activated in the bone marrow microenvironment and is consistent with the lack of TF expression by hematopoietic cells and circulating blood cells. The EMC-LTPRL-DOX was significantly less toxic than doxorubicin when evaluated *in vivo* and its accumulated MTD is greater than 20-fold of that of the doxorubicin (Supplementary Table S3).

### The coagulation activated prodrugs are affective against tumor

The 4T1 murine mammary carcinoma model was used to evaluate the efficacy and safety of Peg-LTPRL-DOX, EMC-LTPRL-DOX, and doxorubicin. On 21-day posttreatment, tumor volumes of the prodrug-treated groups (3  $\mu\text{mol}/\text{kg}$ ) were significantly smaller than the control group (Fig. 6A;  $P < 0.01$  for EMC-LTPRL-DOX,  $n = 6$ ). The MTD of Peg-LTPRL-DOX (i. p. 5 $\times$ ) was greater than 54  $\mu\text{mol}/\text{kg}$  versus that of DOX at 2.8  $\mu\text{mol}/\text{kg}$ . Treatment of 4T1 at MTD of DOX showed growth retardation in this model versus untreated control.

### Prodrug with the EMC tag has enhanced efficacy

The efficacy of the albumin-binding prodrug EMC-LTPRL-DOX was further enhanced (Fig. 6A), compared with Peg-LTPRL-DOX at 3  $\mu\text{mol}/\text{kg}$  dosage and resulted in near complete growth inhibition at 3  $\mu\text{mol}/\text{kg}$ . Thus, prodrug treatment significantly prolonged survival of tumor-bearing mice compared with untreated controls and DOX-treated groups (Fig. 6B). Both prodrug treatments caused massive tumor death upon histologic analysis (Supplementary Fig. S3). In groups treated with EMC-LTPRL-DOX at a higher dose, the tumor growth was completely halted and started to reduce upon continued treatment (Fig. 6C). Importantly, in a human MBA-MD-231 xenograph model, EMC-LTPRL-DOX treatment at 3  $\mu\text{mol}/\text{kg}$  led to complete tumor eradication and non-recurrence with no weight loss and no other apparent signs of toxicity (Fig. 6D).

### Albumin bound prodrug eliminates established breast cancer metastasis in lung

EMC-LTPRL-DOX treatment at 3  $\mu\text{mol}/\text{kg}$  has significant inhibitory effects on spontaneous metastasis of 4T1 murine mammary carcinoma (Fig. 7A and B). H&E staining of lung sections showed metastasis and extensive lung architecture destruction in untreated control mice, whereas in the treated mice, metastasis was significantly inhibited and the lung architecture was nearly normal (Fig. 7C).

Next, we evaluated the effect of high-dosage treatment on established metastasis. The lung metastasis was induced by i.v. injection of 4T1 murine mammary carcinoma cells. On day 16, tumor metastasis was already established in the lung of tumor-bearing animals (Fig. 7D, control 16 days). The high dose EMC-LTPRL-DOX treatment was initiated on day 16 with

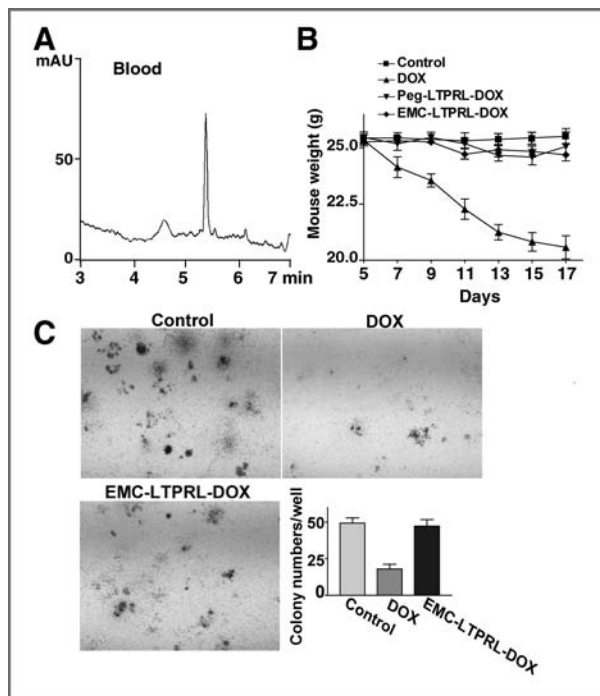
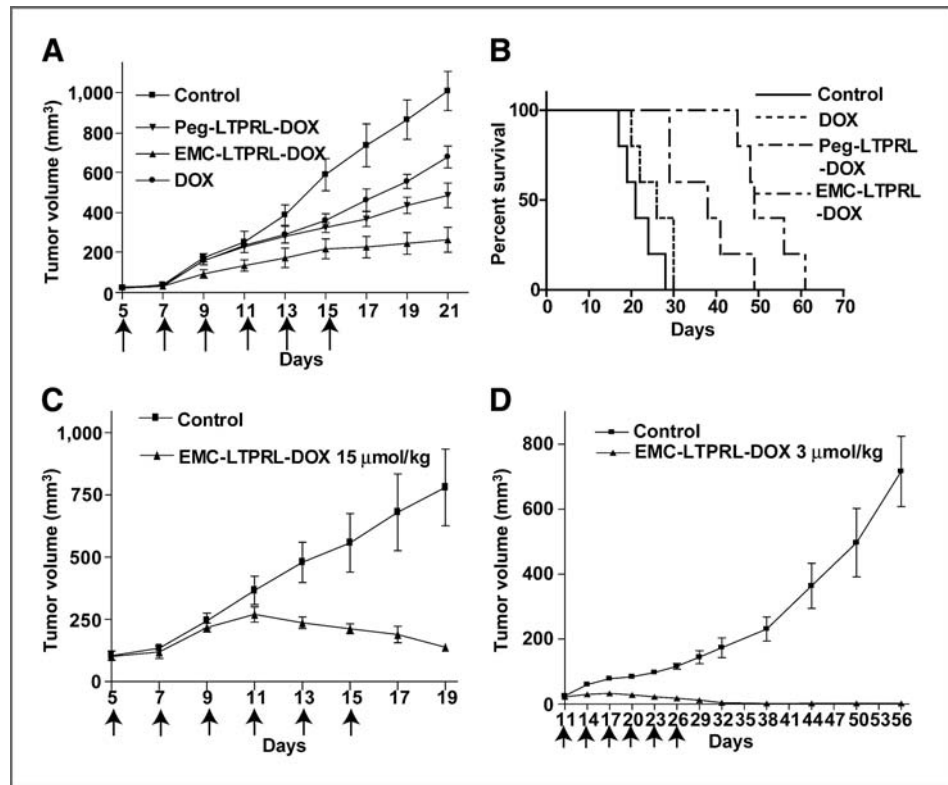


**Figure 5.** EMC-LTPRL-DOX prodrug has favorable *in vivo* properties and low toxicity. A, liquid chromatography of Peg-LTPRL-DOX incubated with serum. B, weight loss of mice-treated prodrugs and doxorubicin. C, colony formation assay.

**Figure 6.** Tumoricidal effect of prodrugs in mammary carcinoma. **A**, *in vivo* effect of low-dose treatment of prodrugs on 4T1 carcinoma. ( $6 \times$  i.p.  $3 \mu\text{mol/kg}$ ) and Kaplan–Meier survival curves (**B**). **C**, *in vivo* effect of high-dose treatment of EMC-LTPRL-DOX on 4T1 carcinoma. ( $6 \times$  i.p.  $15 \mu\text{mol/kg}$ ,  $P < 0.001$ ). **D**, *in vivo* effect of EMC-LTPRL-DOX on MDA-MB231 carcinoma. ( $6 \times$  i.p.  $3 \mu\text{mol/kg}$ ;  $P < 0.001$ ).



$10 \mu\text{mol/kg}$  dose for 7 injections. The lungs were dissected on day 25. Lung metastasis of the treated group on day 25 was compared with that of the control on day 16 (Fig. 7D). The lung metastasis in the EMC-LTPRL-DOX-treated group on day 25 was significantly less than that found in control mice on the day 16 indicating the high dose EMC-LTPRL-DOX treatment is capable of eliminating established lung metastasis in these mice (Fig. 7E). H&E staining of lung sections revealed that treatment of metastasis greatly improves lung tissue morphology (Fig. 7F). Elimination of established metastasis is a very challenging assay and has great clinical relevance. Taken together, the effect of EMC-LTPRL-DOX represents a promising treatment for metastatic cancer, a major cause of mortality of cancer patients.

## Discussion

TF is overexpressed in many types of human cancers, and clinical studies have shown a correlation between the levels of TF expression and poor prognosis (22–25). Not only does TF expression occur in a wide spectrum of cancers, but also the level of expression in cancer cells is upregulated by 1,000-fold compared with the levels of normal cells that these cancer cells are derived from (26, 27). This drastic upregulation may, to some extent, be caused by the existence of common tumor microenvironmental stimuli, such as those responsible for TF upregulation during inflammation and hypoxia. Recently, it was shown that TF expression is under the direct control of oncogenic pathways activated by genetic mutations sustained by cancer cells (28). This is shown experimentally by the effect

of several mutant oncogenes, including K-ras, EGFR, EGFRvIII, HER-2, and PML-RAR $\alpha$  on TF transcription, translation, half-life, and encryption. The effect of these oncogenes was operative in colorectal, mammary, cutaneous, and astrocytic cancer cells (28–31). In addition, similar changes are also found in loss of function mutations of major tumor suppressor genes such as p53 and PTEN (2, 30–32).

Several recent studies indicate that TF plays a role in tumor biology (33). The formation of the TF:FVIIa and TF:FVIIa:FXa complexes leads to cleavage of protease-activated receptors (PAR) at the cell surface (34). The TF:FVIIa–PAR-2 pathway induces expression of the proangiogenic cytokine IL-8 in tumor cells (35) and also contributes to retinal neoangiogenesis (36). The TF cytoplasmic domain can regulate the p38 mitogen-activated kinase and extracellular signal-regulated kinase1/2 and the rac pathways (37) as well as suppress integrin-mediated migration of cells (36). Increased intravascular TF expression is observed in cancers (33, 38). TF is also expressed by tumor cells as well stromal cells such as monocytes, macrophages, and endothelial cells (38). This may contribute to the prothrombotic state (Trousseau's syndrome) associated with a high percentage of cancer patients (27). In addition, TF containing procoagulant microparticles may be shed from different cells, including platelets, leukocytes, and endothelial cells, or from cancer cells (39–44) and recently these particles were shown to be important to tumor growth (4).

Breeding conditional TF knockout mice with PyVmT murine spontaneous mammary carcinoma model, we generated for the first time conditional TF knockout tumor lines that are tumorigenic and metastatic in C57Bl/6 mice. Multiple stable



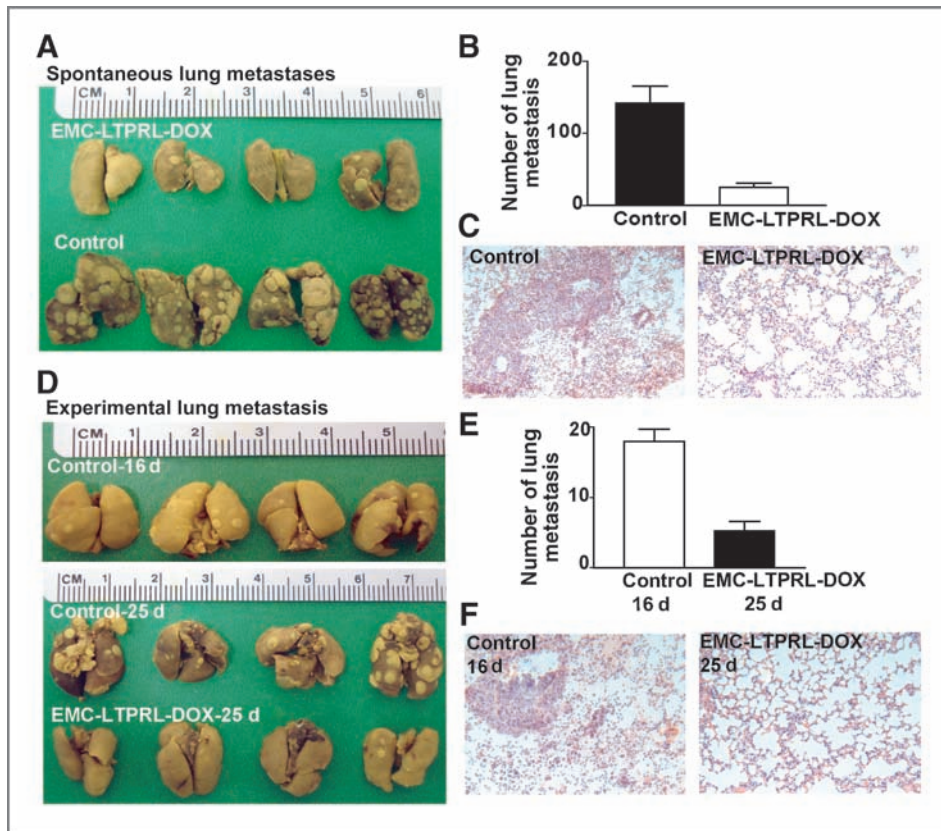


Figure 7. EMC-LTPRL-DOX eliminates established lung metastasis. Representative lung specimens (A), number ( $P < 0.001$ ; B), and H&E staining (C) of spontaneous lung metastasis in 4T1 models. Representative lung specimens (D), number ( $P < 0.001$ ; E), and H&E staining (F) of experimental lung metastasis in 4T1 models. Metastatic sites are already established at day 16 and are eliminated at day 25 by treatment with EMC-LTPRL-DOX.

cancer lines were established from this tumor model. They express a high level of TF and the TF gene can be removed by Cre expressing adenovirus *in vitro*. The growth patterns of the TF wild type and the TF-deficient cancer cells provided clear evidence that TF expressed by tumor cells is required for the accelerated growth of cancers in this model. In contrast, the growth of tumor cells in mice lacking TF either in myeloid-derived cells and endothelial cells is barely affected, suggesting the contribution of TF expressed by these 2 types of stromal cells is small.

Consistent with enhanced permeability of the tumor vasculature, we have shown that coagulation factors are readily extravasated in tumors. Furthermore, TF initiates the activation of the coagulation cascade in the tumor microenvironment.

On the basis of on these findings, we designed and validated PEG-LTPRL-DOX and EMC-LTPRL-DOX prodrugs that can be selectively catalytically converted to the cytotoxic end product by the tissue factor-activated coagulation cascade in the tumor microenvironment. PEG-LTPRL-DOX and EMC-LTPRL-DOX activation is not found in any significant amount in normal tissues because TF:FVIIa and thrombin are not activated without injury. Importantly, PEG-LTPRL-DOX and EMC-LTPRL-DOX are very stable in plasma. We found the little effect of PEG-LTPRL-DOX and EMC-LTPRL-DOX on cells of myeloid lineage, as mice showed a negligible reduction in peripheral blood or marrow myeloid cells at elevated therapeutic doses. Although this therapeutic approach showed little toxicity in our mouse models, the potential toxic risks of off

site activation require careful evaluation in cancer patients especially when persistent thrombotic conditions such as deep vein thrombosis exist. Selection criteria to exclude such higher-risk patients may be necessary in initial clinical trial.

Because of the reduced toxicity, larger cumulative dosage of PEG-LTPRL-DOX and EMC-LTPRL-DOX can be administered more frequently. Consequently, significant effect of EMC-LTPRL-DOX on tumor has been observed in the 4T1 mouse carcinoma model. In high-dose treatment of EMC-LTPRL-DOX in the human MDA-MB231 carcinoma model, the tumor was completely eradicated, and the host survives long term. In high-dose treatment, EMC-LTPRL-DOX not only reduced 4T1 tumor metastasis to lung, but also halted and eradicated established metastasis.

In summary, TF expression in malignant cancers is widely recognized, yet its functions during tumor progression are unknown. Our findings implicate TF expressed by cancer cells can activate a coagulation cascade in the tumor microenvironment and is an essential contributor to tumor progression. For robust and critical hydrolases, including proteases and glycosidases that are enriched and activated in the tumor microenvironment, sufficient inhibition may prove difficult to achieve pharmacologically without significant toxicity. Target the enzymatic activity for prodrug activation is an attractive alternative and amenable to rationally design drug candidates. Development of clinically viable inhibitors for these enzymes has proven to be difficult and has taken up an overwhelming majority of our collective cancer drug

discovery efforts. Herein we showed that eradication of primary and metastatic cancers can be achieved by functionally targeted prodrugs in animal models; our findings provide a logical path for future preclinical and clinical studies of this form of targeted cancer therapy.

### Disclosure of Potential Conflicts of Interest

No potential conflicts of interest were disclosed.

### References

1. Davie EW, Fujikawa K, Kisiel W. The coagulation cascade: initiation, maintenance, and regulation. *Biochemistry* 1991;30:10363–70.
2. Milsom C, Yu J, May L, Magnus N, Rak J. Diverse roles of tissue factor-expressing cell subsets in tumor progression. *Semin Thromb Hemost* 2008;34:170–81.
3. Mueller BM, Ruf W. Requirement for binding of catalytically active factor VIIa in tissue factor-dependent experimental metastasis. *J Clin Invest* 1998;101:1372–8.
4. Palumbo JS, Talmage KE, Massari JV, La Jeunesse CM, Flick MJ, Kombrinck KW, et al. Tumor cell-associated tissue factor and circulating hemostatic factors cooperate to increase metastatic potential through natural killer cell-dependent and-independent mechanisms. *Blood* 2007;110:133–41.
5. Schaffner F, Ruf W. Tissue factor and protease-activated receptor signaling in cancer. *Semin Thromb Hemost* 2008;34:147–53.
6. Versteeg HH, Schaffner F, Kerver M, Petersen HH, Ahamed J, Felding-Habermann B, et al. Inhibition of tissue factor signaling suppresses tumor growth. *Blood* 2008;111:190–9.
7. Bazan JF. WKS motifs and the cytokine receptor framework of tissue factor. *Trends Biochem Sci* 1991;16:329.
8. Edgington TS, Mackman N, Brand K, Ruf W. The structural biology of expression and function of tissue factor. *Thromb Haemost* 1991;66:67–79.
9. Morrissey JH, Fakhrai H, Edgington TS. Molecular cloning of the cDNA for tissue factor, the cellular receptor for the initiation of the coagulation protease cascade. *Cell* 1987;50:129–35.
10. Bauer KA, Kass BL, ten Cate H, Hawiger JJ, Rosenberg RD. Factor IX is activated *in vivo* by the tissue factor mechanism. *Blood* 1990;76:731–6.
11. ten Cate H, Bauer KA, Levi M, Edgington TS, Sublett RD, Barzegar S, et al. The activation of factor X and prothrombin by recombinant factor VIIa *in vivo* is mediated by tissue factor. *J Clin Invest* 1993;92:1207–12.
12. de Groot FM, de Bart AC, Verheijen JH, Scheeren HW. Synthesis and biological evaluation of novel prodrugs of anthracyclines for selective activation by the tumor-associated protease plasmin. *J Med Chem* 1999;42:5277–83.
13. Chakravarty PK, Carl PL, Weber MJ, Katzenellenbogen JA. Plasmin-activated prodrugs for cancer chemotherapy. 2. Synthesis and biological activity of peptidyl derivatives of doxorubicin. *J Med Chem* 1983;26:638–44.
14. Satchi R, Connors TA, Duncan R. PDEPT: polymer-directed enzyme prodrug therapy. I. HPMA copolymer-cathepsin B and PK1 as a model combination. *Br J Cancer* 2001;85:1070–6.
15. Dubowchik GM, Firestone RA. Cathepsin B-sensitive dipeptide prodrugs. 1. A model study of structural requirements for efficient release of doxorubicin. *Bioorg Med Chem Lett* 1998;8:3341–6.
16. Parker KA, Tollefsen DM. The protease specificity of heparin cofactor II. Inhibition of thrombin generated during coagulation. *J Biol Chem* 1985;260:3501–5.
17. Butenas S, DiLorenzo ME, Mann KG. Ultrasensitive fluorogenic substrates for serine proteases. *Thromb Haemost* 1997;78:1193–201.
18. Liu C, Sun C, Huang H, Janda K, Edgington T. Overexpression of legumain in tumors is significant for invasion/metastasis and a candidate enzymatic target for prodrug therapy. *Cancer Res* 2003;63:2957–64.
19. Wu W, Luo Y, Sun C, Liu Y, Kuo P, Varga J, et al. Targeting cell-impermeable prodrug activation to tumor microenvironment eradicates multiple drug-resistant neoplasms. *Cancer Res* 2006;66:970–80.
20. Kratz F, Warnecke A, Scheuermann K, Stockmar C, Schwab J, Lazar P, et al. Probing the cysteine-34 position of endogenous serum albumin with thiol-binding doxorubicin derivatives. Improved efficacy of an acid-sensitive doxorubicin derivative with specific albumin-binding properties compared to that of the parent compound. *J Med Chem* 2002;45:5523–33.
21. Kratz F, Beyer U. Serum proteins as drug carriers of anticancer agents, a review. *Drug Delivery* 1998;5:281–99.
22. Akashi T, Furuya Y, Ohta S, Fuse H. Tissue factor expression and prognosis in patients with metastatic prostate cancer. *Urology* 2003;62:1078–82.
23. Poon RT, Lau CP, Ho JW, Yu WC, Fan ST, Wong J. Tissue factor expression correlates with tumor angiogenesis and invasiveness in human hepatocellular carcinoma. *Clin Cancer Res* 2003;9:5339–45.
24. Shigemori C, Wada H, Matsumoto K, Shiku H, Nakamura S, Suzuki H. Tissue factor expression and metastatic potential of colorectal cancer. *Thromb Haemost* 1998;80:894–8.
25. Ueno T, Toi M, Koike M, Nakamura S, Tominaga T. Tissue factor expression in breast cancer tissues: its correlation with prognosis and plasma concentration. *Br J Cancer* 2000;83:164–70.
26. Mueller BM, Reisfeld RA, Edgington TS, Ruf W. Expression of tissue factor by melanoma cells promotes efficient hematogenous metastasis. *Proc Natl Acad Sci U S A* 1992;89:11832–6.
27. Rickles FR. Mechanisms of cancer-induced thrombosis in cancer. *Pathophysiol Haemost Thromb* 2006;35:103–10.
28. Rak J, Milsom C, May L, Klement P, Yu J. Tissue factor in cancer and angiogenesis: the molecular link between genetic tumor progression, tumor neovascularization, and cancer coagulopathy. *Semin Thromb Hemost* 2006;32:54–70.
29. Tallman MS, Lefebvre P, Baine RM, Shoji M, Cohen I, Green D, et al. Effects of all-trans retinoic acid or chemotherapy on the molecular regulation of systemic blood coagulation and fibrinolysis in patients with acute promyelocytic leukemia. *J Thromb Haemost* 2004;2:1341–50.
30. Yu JL, May L, Klement P, Weitz JI, Rak J. Oncogenes as regulators of tissue factor expression in cancer: implications for tumor angiogenesis and anti-cancer therapy. *Semin Thromb Hemost* 2004;30:21–30.
31. Yu JL, May L, Lhotak V, Shahrzad S, Shirasawa S, Weitz JI, et al. Oncogenic events regulate tissue factor expression in colorectal cancer cells: implications for tumor progression and angiogenesis. *Blood* 2005;105:1734–41.
32. Rong Y, Post DE, Pieper RO, Durden DL, Van Meir EG, Brat DJ. PTEN and hypoxia regulate tissue factor expression and plasma coagulation by glioblastoma. *Cancer Res* 2005;65:1406–13.
33. Pawlinski R, Mackman N. Use of mouse models to study the role of tissue factor in tumor biology. *Semin Thromb Hemost* 2008;34:182–6.
34. Ruf W, Dorfleutner A, Riewald M. Specificity of coagulation factor signaling. *J Thromb Haemost* 2003;1:1495–503.
35. Hjortoe GM, Petersen LC, Albrektsen T, Sorensen BB, Norby PL, Mandal SK, et al. Tissue factor-factor VIIa-specific up-regulation of IL-8 expression in MDA-MB-231 cells is mediated by PAR-2 and results in increased cell migration. *Blood* 2004;103:3029–37.

### Grant Support

This work was financially supported by the US National Cancer Institute (CA127535) and the US Department of Defense (W81XWH-07-1-0389, W81XWH-05-1-0091, W81XWH-05-1-0318, W81XWH-09-1-0690) to C. Liu.

The costs of publication of this article were defrayed in part by the payment of page charges. This article must therefore be hereby marked *advertisement* in accordance with 18 U.S.C. Section 1734 solely to indicate this fact.

Received April 4, 2011; revised August 2, 2011; accepted August 20, 2011; published OnlineFirst August 25, 2011.

36. Belting M, Dorrell MI, Sandgren S, Aguilar E, Ahamed J, Dorfleutner A, et al. Regulation of angiogenesis by tissue factor cytoplasmic domain signaling. *Nat Med* 2004;10:502–9.
37. Ahamed J, Niessen F, Kurokawa T, Lee YK, Bhattacharjee G, Morrissey JH, et al. Regulation of macrophage procoagulant responses by the tissue factor cytoplasmic domain in endotoxemia. *Blood* 2007;109:5251–9.
38. Pawlinski R, Pedersen B, Schabbauer G, Tencati M, Holscher T, Boisvert W, et al. Role of tissue factor and protease-activated receptors in a mouse model of endotoxemia. *Blood* 2004;103:1342–7.
39. Combes V, Simon AC, Grau GE, Arnoux D, Camoin L, Sabatier F, et al. *In vitro* generation of endothelial microparticles and possible prothrombotic activity in patients with lupus anticoagulant. *J Clin Invest* 1999;104:93–102.
40. Dvorak HF, Quay SC, Orenstein NS, Dvorak AM, Hahn P, Bitzer AM, et al. Tumor shedding and coagulation. *Science* 1981;212:923–4.
41. Dvorak HF, Van DeWater L, Bitzer AM, Dvorak AM, Anderson D, Harvey VS, et al. Procoagulant activity associated with plasma membrane vesicles shed by cultured tumor cells. *Cancer Res* 1983;43:4434–42.
42. Martin SJ, Reutelingsperger CP, McGahon AJ, Rader JA, van Schie RC, LaFace DM, et al. Early redistribution of plasma membrane phosphatidylserine is a general feature of apoptosis regardless of the initiating stimulus: inhibition by overexpression of Bcl-2 and Abl. *J Exp Med* 1995;182:1545–56.
43. Mesri M, Altieri DC. Endothelial cell activation by leukocyte microparticles. *J Immunol* 1998;161:4382–7.
44. Zwaal RF, Schroit AJ. Pathophysiologic implications of membrane phospholipid asymmetry in blood cells. *Blood* 1997;89:1121–32.